Max-Planck-Institut
für Mathematik
in den Naturwissenschaften
Leipzig

Complex dynamics and the structure of small neural networks

by

Frank Pasemann

Preprint no.: 38 2001

Complex Dynamics and the Structure of Small Neural Networks

Frank Pasemann
Max-Planck-Institute for Mathematics in the Sciences
D-04103 Leipzig, Germany
email: f.pasemann@mis.mpg.de

Abstract

The discrete-time dynamics of particular two and three neuron networks is studied with respect to non-trivial bifurcation scenarios. Interesting dynamical properties like periodic, quasi-periodic and chaotic attractors are observed, many of them coexisting for one and the same set of parameters. Symmetries in parameter space leading to equivalent dynamics are considered. Conditions on the connectivity of these small netwoks, involving excitation as well as inhibition, are derived which admit complex dynamics for these systems.

1 Introduction

For biological brains anatomical as well as physiological observations indicate that neurons are grouped together into functional circuits, and that certain small neural populations can be assumed to represent basic building blocks of a modular organization of brains [1], [3], [29], [38]. Although such hypothesized modules, like the hyper-columns [32], can be composed of as many as 10^5 neurons, already 2-neuron circuits like the recurrent inhibitory loop [17], [36], [39] or 3-neuron circuits, serving, for instance, as central pattern generators [11] are considered to represent the basic feedback mechanisms regulating neural activity in biological brains.

The widespread recurrent structures found in biological neural networks imply the possibility of complex neural dynamics and, in fact, oscillatory and chaotic activity has been observed frequently in brains [9], [12], [13], [20]. This suggests that complex dynamics may play an important role for specific functions of the brain. Therefore these dynamical properties have found steadily increasing attention in recent years; but it still remains an open question to which extent and through what kind of mechanisms oscillatory and chaotic dynamics can contribute to effective signal processing in the brain.

It seems obvious that also artificial neural networks with higher information processing capabilities will be build from a large collection of neurons, and a modular structure of these systems suggests itself. Following such a modular approach implies the attempt to understand the emergent dynamical properties of such a network in terms of interacting smaller subnetworks. Thus, it is considered as a rational first step to study small networks, called neuromodules in the following for obvious reasons, which already exhibit a complex dynamical behavior. In various articles the dynamics of 2- and 3-neuron networks has been studied for different paradigms of artificial networks, for time-continuous systems as well as for the time-discrete case, for spiking neurons as well as for formal neurons [4], [18], [30], [37], [6], [10], [7], [5], [24], [25], [19], [8], [16], [35]. Often the time-discrete dynamics of small recurrent networks has been investigated because their dynamics is easy to simulate, and their observed dynamical properties can be assumed to exist also in corresponding higher-dimensional time-continuous dynamical systems.

Of interest therefore are parameter domains, for which non-convergent dynamics of the neuromodules has to be expected; i.e. we are looking for domains for which there exist periodic or chaotic attractors. Thus, not only a fixed point analysis has to be done here, but the crucial data are obtained by the corresponding bifurcation sets in parameter space. A complete fixed

point analysis for recurrent 2-neuron networks has been given e.g. in [5] for the time-continuous case and in [35] for the time-discrete case.

This paper concentrates on the bifurcation structure of 2- and 3-neuron recurrent networks. They are composed of standard additive neurons having a strictly positive sigmoidal transfer function, and they will be considered as parameterized discrete-time dynamical systems. Relevant parameters are given by the strength of synaptic connections, the bias terms of neurons, and stationary or slowly varying external inputs, respectively. It is assumed that the connectivity structure of modules satisfies Dale's rule; i.e., a given neuron has the same type of action at all its synapses, or otherwise stated, its outgoing connections are all either positive (excitatory) or negative (inhibitory). Correspondingly, a neuron is said to be excitatory or inhibitory. Although this rule is not always realized in biological networks, it will be used here as a simplifying paradigm for the organization of networks.

In the following studies emphasis is layed on chaotic dynamics, not because it is assumed that chaotic dynamics will play an essential role for functional neural processing, but because of the following fact: If a neural circuit allows for parameter values such that chaotic behavior is observed, then in general there also exist parameter values for any kind of periodic behavior (including, of course, also fixed point attractors). In this sense, these so called *chaotic neuromodules* provide a large reservoir of dynamical properties. From this reservoir, a learning algorithm or convenient external driving signals may select those parameter values which lead, perhaps in cooperative interaction with other neuromodules of the system, to a desired or appropriate functional behavior.

A second point which should be emphasized here, is the fact, that for fixed parameter values neuromodules can have different non-trivial attractors at the same time; for instance, a p-periodic attractor may co-exist with a chaotic attractor. Thus it depends on the initial conditions which asymptotic behavior is finally observed. Co-existence of different attractors may lead also to the observation of what has been called a *generalized hysteresis* phenomenon [24]:

If a path of slowly varying parameters is crossing a bifurcation set, it depends on the direction of the path, leaving or entering a hysteresis domain, if there is a sudden jump in the qualitative behavior of the system or not. A path in parameter space crossing the whole hysteresis domain in both directions will cause such jumps at different parameter values, generating a *hysteresis loop* in the state space. In the simplest case, referring to bistability of a system with two parameters, this phenomenon is associated with the so called cusp catastrophe [33], [28], [21]. As is shown in the following, already 2-neuron networks have coexisting non-trivial attractors, like periodic

attractors existing together with quasiperiodic or chaotic ones, and in 3-neuron networks also co-existing chaotic attractors can be observed.

Finally, we want to point out, that with respect to the neurodynamics approach to cognitive systems [27], we understand attractors only as classifying instruments. For neural networks serving as embodied cognitive systems, for example as neuro-controllers acting in a sensori-motor loop, the dynamics always will be that of a driven system. Of relevance for the behavior of such biological or artificial embodied systems is only the structure of the basins of attraction in their phase space. Or otherwise stated, what relates to a specific functional brain process are the transients in one and the same basin of attraction, not specific orbits in the state space of the system, especially not the attractor itself. Of course, the number, structure and size of basins, as well as their defining attractors, are controlled by the parameters of the neuromodules. Thus, different modes of behavior may appear or disappear while crossing corresponding bifurcation sets.

The following section will give a short introduction to neurodynamics and section 3 and 4 will illustrate these ideas with some simple examples of 2- and 3-neuron networks.

2 Discrete-time Neurodynamics

In this section we will describe an n-neuron module, or n-module for short, as a parameterized n-dimensional discrete-time dynamical system $(\mathcal{A}, f_\rho, \mathcal{Q})$ on an n-dimensional activity phase space $\mathcal{A} \subset \mathbf{R}^n$, where the map $f_\rho : \mathcal{A} \to \mathcal{A}$, $\rho \in \mathcal{Q}$ is given by the equation

$$a_i(t+1) = \theta_i + \sum_{j=1}^{n} w_{ij}\, \sigma(a_j(t)) \;, \quad i = 1, \ldots, n \;. \tag{1}$$

Here a_i denotes the activity of unit i, w_{ij} denotes the synaptic weight from unit j to unit i, and $\theta_i = \overline{\theta}_i + I_i$ denotes the sum of its fixed bias term $\overline{\theta}_i$ and its stationary external input I_i. The output $o_i = \sigma(a_i)$ of the units is given by the sigmoidal transfer function

$$\sigma(a) := \frac{1}{1+e^{-a}} \;. \tag{2}$$

Furthermore, $\mathcal{Q} \subset \mathbf{R}^q$ denotes the parameter space, and $\rho \in \mathcal{Q}$ the q-dimensional parameter vector with components $\theta_1, \ldots, \theta_n$ and $w_{11}, \ldots, w_{nn}$. The module dynamics (1) is always dissipative and bounded on an open domain $\mathcal{U} \subset \mathcal{A}$ with bounds given by

$$\theta_i - \sum_{j=1}^{n} |w_{ij}^-| \;\; < a_i < \;\; \theta_i + \sum_{j=1}^{n} w_{ij}^+ \;, \tag{3}$$

where $w_{ij}^+ = w_{ij}$ iff $w_{ij} > 0$, $w_{ij}^- = w_{ij}$ iff $w_{ij} < 0$, and $w_{ij}^\pm = 0$ else.

As explained in the introduction we are mainly interested in network configurations for which complex dynamics has to be espected; i.e. we want to study parameter domains for which there exist interesting bifurcation scenarios like period-doubling routes to chaos, bifurcations from stable fixed points to higher-periodic or quasi-periodic attractors, and the like. To find such parameter domains is in general a difficult analytical task, and usually this will be done with the help of simulation techniques. But in the following we will be guided by the idea that at least one neuron in the network has to receive an excitatory as well as an inhibitory input. Before formulating this idea more precisely we will consider some simple operations on neuromodules.

We define the *flip operators* $I_k : \mathcal{A} \to \mathcal{A}$, $k = 1, \ldots, n$ acting on the k-th component of a state vector $a \in \mathcal{A}$ as a sign reflection; i.e.,

$$(I_k a)_j = \begin{cases} a_j & \text{iff} \quad k \neq j \\ -a_j & \text{iff} \quad k = j \end{cases} \tag{4}$$

Recall, that two dynamical systems $(\mathcal{A}, f)$, $(\mathcal{B}, g)$ are called *topologically conjugate*, iff there exists a homeomorphism $h : \mathcal{A} \to \mathcal{B}$, such that $g \circ h = h \circ f$. Using the symmetry of the sigmoid (2), given by $\sigma(-x) = (1 - \sigma(x))$, it is then easy to prove by direct calculation that for every neuro-module with n neurons there exists a set of 2^n parameter vectors, all leading to qualitatively equivalent dynamical behavior. We have

Lemma 1 *Given an n-neuro-module $(\mathcal{A}, f_\rho)$, $\rho \in \mathcal{Q} \subset \mathbf{R}^q$. If the activity dynamics (1) of a neuro-module is changed by a sign reflection operator I_k, then there exists an induced transformation $\varphi(I_k) = T_k : \mathcal{Q} \to \mathcal{Q}$ on the parameter space $\mathcal{Q}$, such that with $\rho' := T_k(\rho)$ the dynamical system $(\mathcal{A}, f_{\rho'})$ is topological conjugate to $(\mathcal{A}, f_\rho)$; i.e., the following diagram commutes*

$$\begin{array}{ccccc} & & f_\rho & & \\ & \mathcal{Q} \times \mathcal{A} & \longrightarrow & \mathcal{A} & \\ T \times \varphi & \downarrow & & \downarrow & \varphi \\ & \mathcal{Q} \times \mathcal{A} & \longrightarrow & \mathcal{A} & \\ & & f_{\rho'} & & \end{array}$$

The action of the transformations T_k on the parameters is given as follows

$$(T_k\, \theta)_i = \begin{cases} \theta_i + w_{ik} & \text{iff} \quad k \neq i \\ -\theta_i - w_{ii} & \text{iff} \quad k = i \end{cases}, \tag{5}$$

$$(T_k\, w)_{ij} = \begin{cases} -w_{ij} & \text{iff} \quad k = i \quad \text{or} \quad k = j \\ w_{ij} & \text{else} \end{cases}, \tag{6}$$

We will call the associated transformations $\varphi(I_k) = T_k$ also *flip operators* on the parameter space $\mathcal{Q}$. Equations (5), (6) show that $\varphi(I_k) = T_k$ simultaneously changes the sign of all input and output connections of neuron k, except a self-connection, which is invariant under $\varphi(I_k)$.

We now want to come back to our guiding idea that complex dynamics has to be expected if at least one neuron receives an excitatory as well as an inhibitory input. To be more precise we formulate this criterion as follows:

Given an n-dimensional parameterized discrete-time dynamical system $(\mathcal{A}, f_\rho, \mathcal{Q}$ bounded to a domain $\mathcal{U} \subset \mathcal{A}$, and let Df_ρ denote the Jacobian of this system. Then $(\mathcal{A}, f_\rho)$ can display complex dynamics in the above sense, if there exists a parameter vector $\rho \in \mathcal{Q}$ and a state $a^* \in \mathcal{U}$ such that at least for one row i of the linearization by Df_ρ the row sum is zero, i.e.

$$\sum_{j=1}^{n} (Df_\rho)_{ij}\,(a^*) = 0\ . \tag{7}$$

This criterion is suggested by the many observations we made by simulating the dynamics of recurrent networks. But in the light of lemma 1 we know that the dynamics does not change qualitatively if we change the sign of all input and output connections (without a possible self-connection) to a neuron simultaneously. Because rows and columns of the Jacobian Df_ρ seem to play an interesting role, and we may refer to them as vectors and co-vectors, respectively, we define the following objects.

The *i-th in-field* on $\mathcal{A}$ is defined as vector field Z_i on $\mathcal{A}$ with components given by the row elements of the linearization Df_ρ, and the *i-th out-field* on $\mathcal{A}$ is defined as differential 1-form ω_i on $\mathcal{A}$ with components the components of the i-th column of Df_ρ; i.e.

$$Z_i(a) := (w_{i1}\,\sigma'(a_1), \ldots, w_{in}\,\sigma'(a_n))\,, \quad a \in \mathcal{A}\,, \tag{8}$$

$$\omega_i(a) := (w_{1i}\,\sigma'(a_i), \ldots, w_{ni}\,\sigma'(a_i))\,, \quad a \in \mathcal{A}\,. \tag{9}$$

The contraction of ω_i on Z_i is a function Inv_i on $\mathcal{A}$, called the *first loop function* of neuron i; i.e.,

$$Inv_i(a) := \sigma'(a_i) \cdot \sum_{j=1}^{n} w_{ij} \cdot w_{ji} \cdot \sigma'(a_j)\,, \quad a \in \mathcal{U}\,, \quad i \quad \text{fixed}\,. \tag{10}$$

According to lemma 1 Inv_i is invariant under the action of flip operators.

Equation (7) turned out to be a good guide to parameter domains were complex dynamics can occur; at least higher-periodic up to quasi-periodic attractors have been found in corresponding networks. But there are examples where this equation holds but still there is no chaos, or at least no

period-doubling route to chaos observed. For the existence of chaos it seems, that in addition to equation (7) the following has to be satisfied: There exists a parameter vector $\rho \in \mathcal{Q}$ and a state $a \in \mathcal{U}$ such that $Inv_i(a) = 0$ holds for the same i as in equation (7). With equation (10) this corresponds to

$$\sum_{j=1}^{n} w_{ij} \cdot w_{ji} \cdot \sigma'(a_j) = 0\,, \quad a \in \mathcal{U}\,. \tag{11}$$

These conditions turned out to be satisfied whenever complex dynamics appeared in the considered cases of two and three dimensional neurodynamics. Here only 1- and 2-loops can be involved. So these equations probably refer to a special case of a more general condition for higher dimensions. Thus, in the following we will always consider networks with excitatory and inhibitory neurons. A few examples will now be discussed.

3 The Chaotic 2-Neuron Module

The simplest neuro-module to discuss is a network of two neurons. In general, its dynamics is given by a 6-parameter family of maps $f_\rho : \mathbf{R}^2 \to \mathbf{R}^2$, $\rho = (\theta_1, w_{12}, w_{11}\theta_2, w_{21}, w_{22}) \in \mathbf{R}^6$, but for simplicity one may set $w_{22} = 0$ for the following. Thus we will discuss the dynamics defined by

$$\begin{aligned} a_1(t+1) &:= \theta_1 + w_{11}\,\sigma(a_1(t)) + w_{12}\,\sigma(a_2(t))\,, \\ a_2(t+1) &:= \theta_2 + w_{21}\,\sigma(a_1(t))\,. \end{aligned} \tag{12}$$

This configuration is known to allow also chaotic dynamics for some parameter values $\rho \in \mathbf{R}^5$ (see for example [24]), and we will therefore call it a *chaotic 2-module*. To test our criteria for complex dynamics we first observe that condition (7) can be satisfied for the first row of the linearization of this neuro-module, i.e.

$$w_{11}\sigma'(a_1) + w_{12}\sigma'(a_2) = 0$$

if only if $w_{11}w_{12} < 0$, because $\sigma' > 0$ is a strictly positive function. Of course the necessary range of activities a_1 and a_2 can be chosen by fixing corresponding bias terms θ_1 and θ_2 conveniently. We will use a self-inhibitory neuron here; i.e. $w_{11} < 0$. The condition (11) reads now

$$w_{11}^2\sigma'\left(a_1\right) + w_{12}w_{21}\sigma'(a_2) \;= 0\,,$$

for some $a \in \mathcal{A}$. This can be satisfied only if $w_{12}w_{21} < 0$, and for respecting Dale's rule we choose $w_{21} < 0$. Thus, we consider the dynamics of a 2-neuron network consisting of an excitatory and an inhibitory unit.

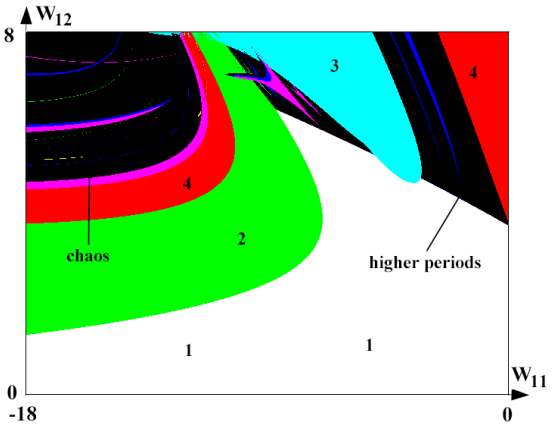

Figure 1: Iso-periodic plot in the (w_{11}, w_{12})-subspace for fixed parameters $w_{21} = -6$, $\theta_1 = -3$, $\theta_2 = 4$.

Without self-connections ($w_{11} = w_{22} = 0$) the resulting recurrent feedback loop has, besides parameter domains for which there exist global fixed point attractors, parameter domains where two fixed point attractors coexist with a period-2 attractor ($w_{12} \cdot w_{21} > 0$), and an other domain where there is a global period-4 attractor ($w_{12} \cdot w_{21} < 0$) [23]. A rough sketch of the complex dynamical properties of the 2-module can be found in the so called iso-periodic plot of figure 1, where color coded we find the periodic attractors existing for corresponding points in the 2-dimensional (w_{11}, w_{12})-parameter subspace.

At this point we may remark that, according to lemma 1, the dynamics of this module is topologically conjugate for the following four parameter vectors :

$$\rho_1 := (\theta_1,\ w_{11},\ w_{12},\ \theta_2,\ w_{21})\ , \tag{13}$$

$$\rho_2 := (-(\theta_1 + w_{11}),\ w_{11},\ -w_{12},\ (\theta_2 + w_{21}),\ -w_{21})\ , \tag{14}$$

$$\rho_3 := ((\theta_1 + w_{12}),\ w_{11},\ -w_{12},\ -\theta_2,\ -w_{21})\ , \tag{15}$$

$$\rho_4 := (-(\theta_1 + w_{11} + w_{12}),\ w_{11},\ w_{12},\ -(\theta_2 + w_{21}),\ w_{21})\ , \tag{16}$$

where $\rho_2 = T_1(\rho_1)$, $\rho_3 = T_2(\rho_1)$, and $\rho_4 = T_1 \circ T_2(\rho_1) = T_2 \circ T_1(\rho_1)$.

Interesting dynamical parameter domains will be those, for which all stationary states are unstable. So we will look for the set of all fixed points a^* such that the Jacobian $Df_\rho(a^*)$ of the dynamics f at a^* has at least one eigenvalue with modulus larger than one. The fixed point equations reads

$$a_i^* = \theta_i + \sum_{j=1}^{2} w_{ij}\, \sigma(a_j^*(t))\ , \quad i = 1, 2\ . \tag{17}$$

and the Jacobian $Df_\rho(a^*)$ of the dynamics (12) with $w_{22} = 0$ is given by

$$Df_\rho(a^*) = \begin{pmatrix} w_{11}\sigma'(a_1^*) & w_{12}\sigma'(a_2^*) \\ w_{21}\sigma'(a_1^*) & 0 \end{pmatrix} . \tag{18}$$

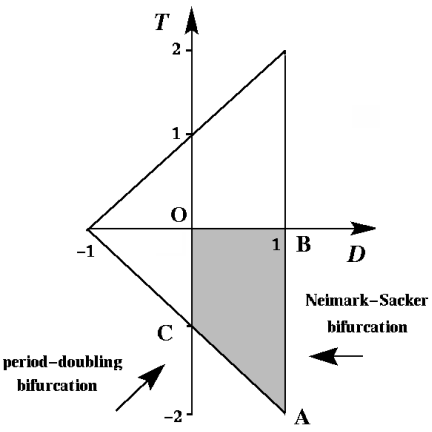

Figure 2: The stability domain for a fixed point in terms of trace $\mathcal{T}$ and determinant $\mathcal{D}$ of the linearization Df_ρ; shaded domain corresponds to recurrent coupling of a self-inhibitory with an excitatory neuron.

We will discuss stability criteria for the stationary states [34] in terms of the trace $\mathcal{T}$ and the determinant $\mathcal{D}$ of $Df_\rho(a^*)$, which are here given by

$$\mathcal{T} = w_{11}\sigma'(a_1^*) , \quad \mathcal{D} = -w_{12}w_{21}\sigma'(a_1^*)\sigma'(a_2^*) .$$

The eigenvalues of $Df_\rho(a^*)$ are then given by

$$\lambda_{1,2} = \frac{1}{2}\left(\mathcal{T} \pm \sqrt{\mathcal{T}^2 - 4\mathcal{D}}\right) .$$

The domain of stability for a fixed point a^* in the $(\mathcal{T}, \mathcal{D})$-plane is given by a triangle bounded by the three straight lines $T - D = 1$, $T + D = -1$, and $D = 1$ [34]. For the case considered here, i.e. $w_{11} \leq 0$, $w_{21} < 0$, and $w_{12} > 0$, we have

$$-|w_{11}| < \mathcal{T} < 0 , \quad 0 < \mathcal{D} < |w_{12}\, w_{21}|\, \sigma'(a_1^*)\, \sigma'(a_2^*) . \tag{19}$$

Thus,at least two types of bifurcations have to be expected: Along the line $\mathcal{T} + \mathcal{D} = -1$ there will be a period-doubling or *flip* bifurcation from a fixed point attractor to a period-2 attractor; along the line $\mathcal{D} = 1$, $|\mathcal{T}| < 2$ there

will be a Neimark-Sacker bifurcation from a fixed point attractor to a periodic or quasiperiodic attractor [34].

In general, the eigenvalues $\lambda_{1,2}\,(a^*)$ are functions not only of the weights w_{ij} but also of the bias terms θ_i, i.e. of all five parameters. This makes a deeper analytical treatment of the bifurcation behavior very difficult [35]. But to get an idea how the structure observed in figure 1 is generated we may look instead for the stability of the origin $(0,0) \in \mathbf{R}^2$ which is a fixed point for parameters satisfying

$$\theta_1 = -\frac{1}{2}\,(w_{11} + w_{12})\;, \quad \theta_2 = -\frac{1}{2}\,w_{21}\;. \tag{20}$$

For this stationary state we get from equations (19) and $\sigma(0) = .5$

$$\mathcal{T} = \frac{1}{4}\,w_{11}\;, \quad \mathcal{D} = -\frac{1}{16}\,w_{12}\,w_{21}\;.$$

So, a flip bifurcation will appear if the weights satisfy the following equations

$$4w_{11} - w_{12}\,w_{21} = -16\;.$$

and the Neimark-Sacker bifurcation will occur for

$$|\,w_{11}\,| < 8\;, \quad |\,w_{12}\,w_{21}\,| = 16\;.$$

To compare these results with the iso-periodic plot in the (w_{11}, w_{12})-plane shown in figure 3, where now in addition to equation (20) we set $w_{21} = -w_{12}$, we obtain for the flip bifurcation set

$$w_{12} = 2\sqrt{-4 - w_{11}}\;, \quad -8 \le w_{11} \le -4\;, \tag{21}$$

and, correspondingly, for the Neimark-Sacker bifurcation set we get the straight line

$$w_{12} = 4\;, \quad -8 < w_{11} < 0\;. \tag{22}$$

The corners of stability domain in the $(\mathcal{D}, \mathcal{T})$-space $O = (0,0)$, $A := (1,-2)$, $B := (1,0)$, $C := (0,-1)$ in figure 2 correspond to the points O', A', B', C' in (w_{11}, w_{12})-parameter subspace of figure 3: Points B, B' correspond to a bifurcation from a fixed point attractor to a global period-4 attractor observed for an odd 2-ring network [23], points C, C' correspond to a single self-inhibitory neuron bifurcating from a stable fixed point to a stable period-2 orbit [21]. Of course, the lines AB and AC of the stability domain $OABC$ are mapped to the bifurcation sets $\overline{A'B'}$ and $\overline{A'C'}$, given by equations (21) and (22), correspondingly.

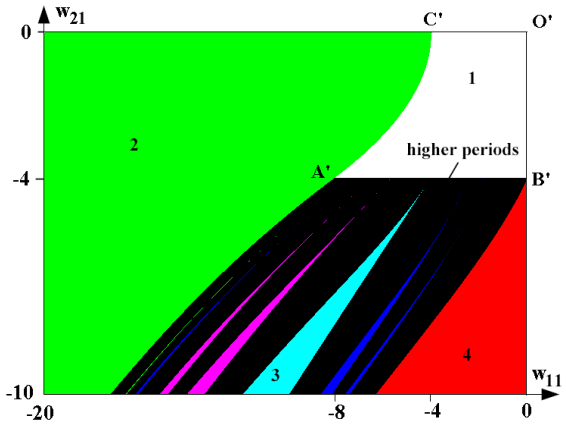

Figure 3: Chaotic 2-module: Iso-periodic plot in the (w_{11}, w_{12})-subspace for $w_{12} = -w_{21}$, $\theta_1 = -0.5\,(w_{11} + w_{12})$, $\theta_2 = -0.5\,w_{21}$. For these parameter values the origin in activity space is always a stationary state.

In general, the components of a fixed point a^* depend on all five parameters of the system [12), and generically they will satisfy $a_i^* \neq 0$, $i, \ldots, n$, i.e. we have $\sigma'(a_i^*) < \sigma'(0) = 0.25$. Thus, the stability domain $O'A'B'C'$ will be smoothly deformed, and, correspondingly, the bifurcation sets $\overline{A'B'}$ and $\overline{A'C'}$ will be smoothly deformed with smoothly varying fixed points a^*. And for $w_{12} = -w_{21}$ complex dynamics will be found only outside of these stability domains.

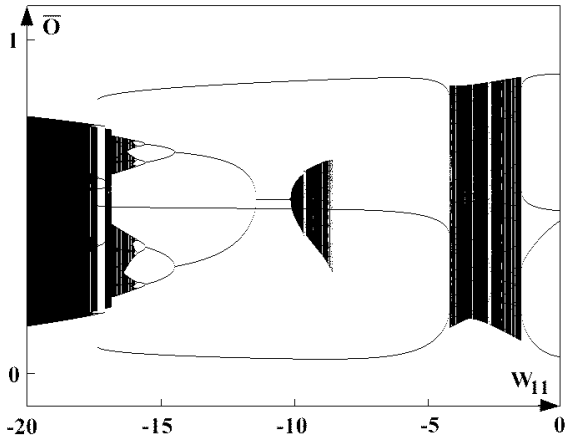

Figure 4: Chaotic 2-module: Bifurcation sequence for w_{11} of the 2-module with $\theta_1 = -3.8$, $\theta_2 = 3$, $w_{12} = 5.9$, $w_{21} = -6.6$.

Especially, figure 1 shows that there exist larger parameter domains where period-3 attractors are dominant. In these period-3 domains there often coexists a whole cascade of period-doubling bifurcations to chaos with a period-3 attractor (compare figure 4). And there are also Neimark-Sacker bifurcations from fixed points to quasiperiodic attractors coexisting with stable period-3 orbits in these domains. These bifurcation diagrams are obtained by multiple passes using different fixed initial conditions. Plotted are the averaged outputs $\overline{o} := \frac{1}{n} \sum_{i=1}^{n} o_i$ of the actual network. For instance, the figure 4 reveals a period-3 attractor coexisting with a period doubling route to chaos in the domain $-17.4 < w_{11} - 11.4$, then a fixed point attractor for $-11.4 < w_{11} < -10.1$ and a domain of quasi-periodic and higher periodic attractors between $-10.1 < w_{11} < -8.5$. A domain of global quasi-periodic and higher periodic attractors exists also between $-4.2 < w_{11} < -1.5$ followed by global period-4 attractors. Noticeable is also a *generalized hysteresis effect* over the whole interval $-17.4 < w_{11} < -1.5$: starting with a chaotic attractor, crossing this hysteresis interval with w_{11} increasing, a period doubling route is followed backward to a fixed point attractor and to quasi-periodic and periodic attractors with the system suddenly jumping into the period-3 attractor. Crossing the interval now again with w_{11} decreasing only the period-3 will appear until the system jumps back to a chaotic attractor around $w_{11} = -17.4$.

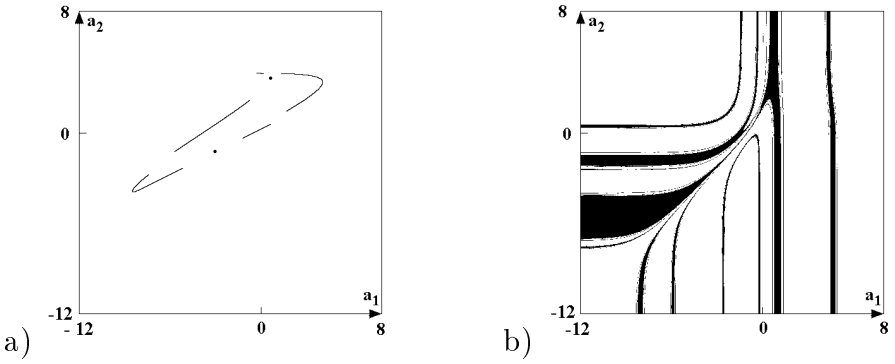

Figure 5: Chaotic 2-module: a.) A period-2 attractor co-existing with a periodic attractor. b.) Basins of period-2 attractor (black) and chaotic attractor (white) for the parameter values $\theta_1 = -0.45$, $\theta_2 = 3.9$, $w_{11} = -16$, $w_{12} = 8$, $w_{21} = -8$.

Although the basin structure of coexisting chaotic and period-3 attractors seems to be quite regular in general, there exist also chaotic attractors together with period-2 orbits, having fractal basin boundaries. An exam-

ple is given in figures 5a and 5b for the parameter values $\theta_1 = -0.45$, $\theta_2 = 3.9$, $w_{11} = -16$, $w_{12} = 8$, $w_{21} = -8$.

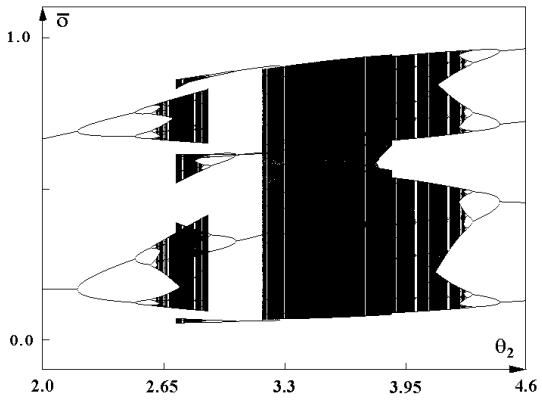

Figure 6: Chaotic 2-module: Bifurcation sequence for θ_2 of the chaotic 2-module with $\theta_1 = -1.74$, $w_{11} = -16, w_{12} = 6$, $w_{21} = -6$.

The existence of even more complex dynamical behavior can be detected in the bifurcation sequence for the parameter θ_2 shown in figure 6; the other parameters are fixed as follows: $\theta_1 = -1.74$, $w_{11} = -16$, $w_{12} = 6$, $w_{21} = -6$. To analyze this situation recall, that a chaotic attractor is called *p-cyclic*, if it has p connected components which are permuted cyclically by the map f_ρ. Every component of a p-cyclic attractor is an attractor of the p-th iterate f_ρ^p [2].

Now, over the interval $2.72 < \theta_2 < 2.9$ there coexist two different chaotic attractors. One is 2-cyclic, the other is 5-cyclic. Both are shown in figure 7a. Thus, over this interval we observe a generalized hysteresis effect, switching between two different cyclic chaotic behaviors. A second hysteresis interval $3.18 > \theta_2 > 3.28$ can be seen, where a chaotic attractor coexists with a period-5 attractor. This configuration is depicted in 7b.

4 Three Neuron Modules

In this section we will discuss different types of 3-neuron modules. According to our guide line, for producing interesting dynamical properties these modules should have at least one neuron getting excitatory as well as inhibitory inputs. This can be realized, for example, by the three configurations shown in figure 8. The first one has a self-inhibiting neuron in the middle of a bi-directional 3-chain. The second one uses an inhibitory neuron at one end

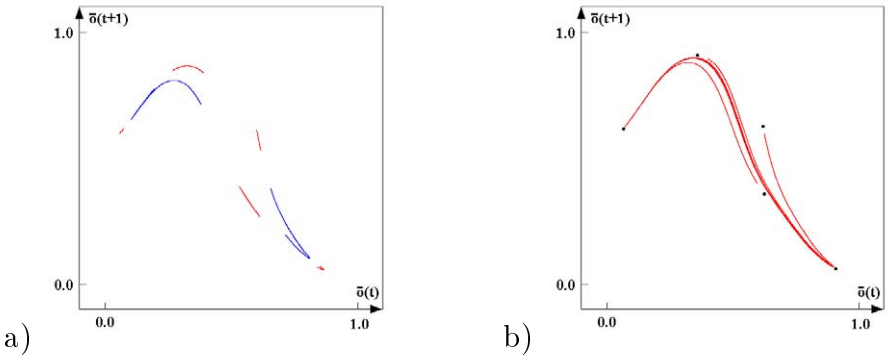

Figure 7: Chaotic 2-module: for parameters $\theta_1 = -1.75$, $w_{11} = -16$, $w_{12} = 6$, $w_{21} = -6$ one observes a.) a 2-cyclic chaotic attractor coexisting with a 5-cyclic one for $\theta_2 = 2.78$, and b.) a chaotic attractor coexisting with a period-5 attractor for $\theta_2 = 3.25$.

of such a chain. The third configuration is a bi-directional 3-ring with one inhibitory neuron. All these configurations can display chaotic dynamics.

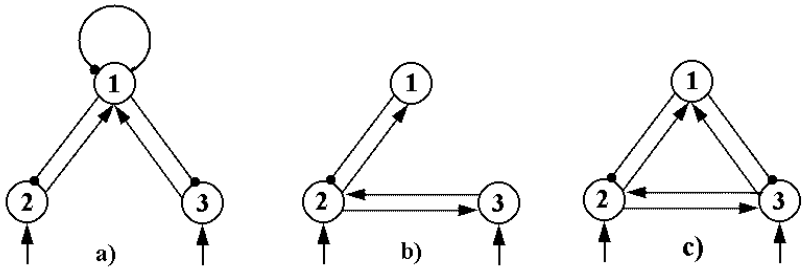

Figure 8: Three 3-neuron modules, both with one inhibitory neuron. Arrows denote excitatory, dots inhibitory connections.

4.1 3-chain with self-inhibiting center neuron

This module is described as a discrete-time dynamical system with eight parameters given by

$$\begin{aligned} a_1(t+1) &:= \theta_1 + w_{11}\,\sigma(a_1(t) + w_{12}\,\sigma(a_2(t)) + w_{13}\,\sigma(a_3(t))\,, \\ a_2(t+1) &:= \theta_2 + w_{21}\,\sigma(a_1(t))\,, \\ a_3(t+1) &:= \theta_3 + w_{31}\,\sigma(a_1(t))\,. \end{aligned} \tag{23}$$

To go to dynamically interesting parameter domains for this configuration the first condition (7) of the complex dynamics criterion

$$w_{11}\sigma'(a_1) + w_{12}\sigma'(a_2) + w_{13}\sigma'(a_3) = 0$$

can be satisfied if we assume for the first row of the linearization $w_{11} < 0$ and $w_{12}\,, w_{13} > 0$. Then the bias terms can again be arranged in such a way, so that this condition holds. The chaos condition (11) now reads

$$Inv_1 = w_{11}^2\sigma'(a_1) + w_{12}w_{21}\sigma'(a_2) + w_{13}w_{31}\sigma'(a_3) \; = 0 \;,$$

for some $a \in \mathcal{A}$. This can be satisfied only if $w_{12}w_{21} < 0$ and/or $w_{13}w_{23} < 0$, and for respecting Dale's rule we choose $w_{21},\; w_{31} < 0$. Thus, we consider the dynamics of a self-inhibiting neuron coupled bi-directionally to two excitatory neurons as shown in figure 8a.

It can be easily shown that the 3-dimensional dynamics (23) is essentially a 2-dimensional one, living on a 2-dimensional sub-manifold in 3-dimensional activity space $\mathcal{A}$. This is the case, because neurons 2 and 3 are synchronized in the general sense [22]; i.e. their activities are related by the equation:

$$a_3(t) = \theta_3 + \frac{w_{31}}{w_{21}}(a_2(t) - \theta_2) \;. \tag{24}$$

Although the 3-module (23) is effectively a 2-dimensional systems, it can of course not be reduced to a 2-neuron network. This can be done only in the special case, for which the excitatory neurons 2 and 3 are synchronized, i.e. $a_2(t) = a_3(t)$ for all $t > t_0$. This is realized iff the following *synchronization condition* is satisfied:

$$\theta_2 = \theta_3, \quad w_{21} = w_{31} \;. \tag{25}$$

Then the dynamics (23) of the module reduces to the dynamics (12) of a two neuron network A having a connection $w_{12}^A = (w_{12} + w_{13})$.

Suppose the eight parameters of the dynamics (23) satisfy

$$-2\,\theta_1 = (w_{11} + w_{12} + w_{13}) \;, \quad -2\,\theta_2 = w_{21} \;, \quad -2\,\theta_3 = w_{31} \;. \tag{26}$$

Then the origin $a^* = (0, 0, 0)$ is a stationary state, and the eigenvalues of the linearization $Df_\rho(a^*)$ at a^* are given by

$$\lambda_1(0) \;, \quad \lambda_{2,3}(0) = \frac{1}{8}\,(w_{11} \pm \sqrt{w_{11}^2 - \,4\,(w_{12}w_{21} + w_{13}w_{31})}) \;.$$

This stationary state will become non-hyperbolic if one of these eigenvalues has modulus 1. Because $w_{12}w_{21} < 0$ and $w_{13}w_{31} < 0$ (both loops are odd)

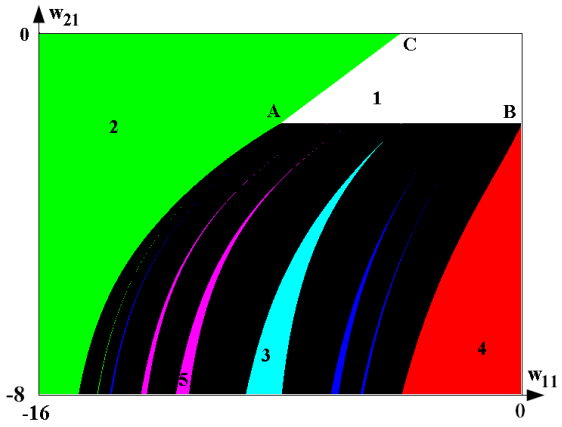

Figure 9: 3-chain 4.1: Iso-periodic plot in the (w_{11}, w_{21})-parameter subspace for which the origin $a^* = 0$ is always a fixed point (see text for parameters).

there will be only real eigenvalues, and the bifurcation sets in parameter space are defined by

$$16 + (w_{12}w_{21} + w_{13}w_{31}) \pm 4\,w_{11} = 0\ .$$

For the special case where in addition to equations 26 parameters satisfy also $w_{21} = w_{31}$ and $w_{12} = w_{13} = 4$, an iso-periodic plot in the (w_{11}, w_{21})-parameter subspace is depicted in figure 12. In this figure the line $\overline{AC}$ correspond to period -doubling bifurcations, the line $\overline{AC}$ to Neimark-Sacker bifurcations. Points have coordinates $A = (-8, -2)$, $B = (0. - 2)$, $C = (-4, 0)$. Because the dynamics of the module is essentially a 2-dimensional one - as was stated above - this figure is clearly equivalent to that of the 2-module in figure 3.

According to lemma 1, there are now in general 8 different parameter vectors $\rho \in \mathbf{R}^8$ generated by the basic transformation T_k, $k = 1, 2, 3$, all giving topologically conjugate dynamics. Knowing that for $\theta_2 = \theta_3$, $w_{21} = w_{31}$ the module dynamics reduces to the known 2-dimensional one, we may ask what happens if $\theta_2 \neq \theta_3$. So, for a first simulation, shown again in terms of an iso-periodic plot for the (θ_2, θ_3)-parameter space in figure 10, we choose $w_{12} = w_{13} = 4$, $w_{21} = w_{31} = -6$, $w_{11} = -16$, and $\theta_1 = -3.4$.

We observe that the 3-dimensional dynamics around the main diagonal, which corresponds to the synchronization condition (25) for neurons 2 and 3, has qualitatively the same properties as the chaotic 2-neuron module: Besides fixed point attractors, we have large domains for period-2 and period-3 attractors, period doubling routes to chaos, also co-existing with period-3

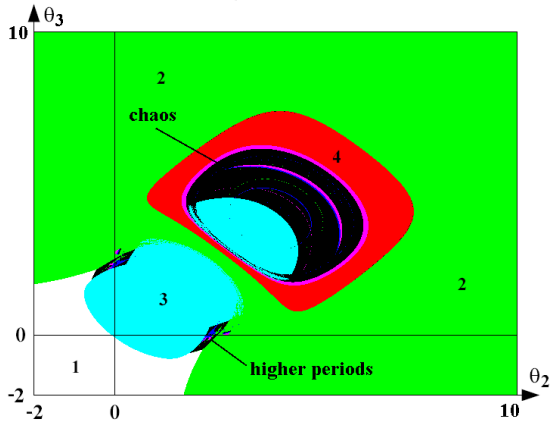

Figure 10: 3-chain 4.1: Iso-periodic plot for (θ_2, θ_3)-parameter space for $w_{12} = w_{13} = 4$, $w_{21} = w_{31} = -6$, $w_{11} = -16$, $\theta_1 = -3.4$ fixed.

attractors in the middle of the figure, and domains for higher periodic and quasi-periodic attractors crossing the θ_1- and θ_2-axis.

The synchronization condition (25) is violated for the situation depicted in figure 11 where an iso-period plot in the (θ_2, w_{21})-parameter space is shown for $\theta_1 = -2$, $\theta_3 = 3.4$, $w_{11} = -16$, $w_{21} = w_{31} = -6$, $w_{13} = 4$. Again we find the typical dynamical properties like period-doubling routes to chaos, higher- and quasi-periodic attractors and large period-3 domains as described before.

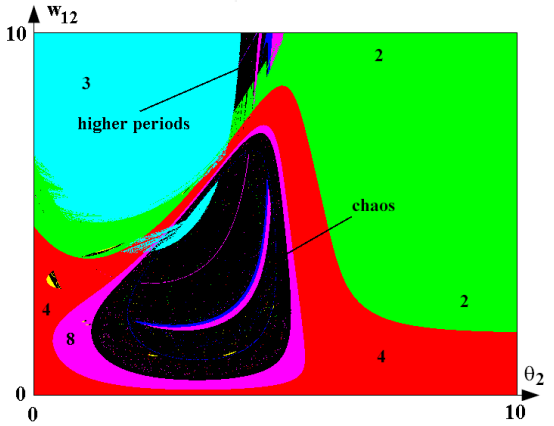

Figure 11: 3-chain 4.1: Iso-periodic plot or (θ_2, w_{21})-parameters with $\theta_1 = -2$, $\theta_3 = 3.4$, $w_{11} = -16$, $w_{21} = w_{31} = -6$, $w_{13} = 4$ fixed.

4.2 3-chain with inhibitory neuron at one end

The second 3-neuron module corresponds to a bi-directional 3-chain with an inhibitory neuron at one end (figure 8b). Its discrete dynamics is given by a seven parameter family of maps $f_\rho : \mathbf{R}^3 \to \mathbf{R}^3$ defined by

$$\begin{aligned} a_1(t+1) &:= \theta_1 + w_{12}\,\sigma(a_2(t)) \;, \\ a_2(t+1) &:= \theta_2 + w_{21}\,\sigma(a_1(t)) + w_{23}\,\sigma(a_3(t)) \;, \\ a_3(t+1) &:= \theta_3 + w_{32}\,\sigma(a_2(t)) \;. \end{aligned} \tag{27}$$

A complex dynamics condition (7) for this configuration is given for neuron 2 by

$$w_{21}\sigma'(a_1) + w_{23}\sigma'(a_3) = 0 \;,$$

and it can be satisfied with $w_{21}w_{23} < 0$ by adjusting the corresponding bias terms. In the following we choose neuron 1 to be inhibitory, i.e., $w_{21} < 0$. The chaos condition (11) for the second component reads

$$Inv_2 = w_{12}w_{21}\sigma'(a_1) + w_{23}w_{32}\sigma'(a_3) \;= 0 \;,$$

for some $a \in \mathcal{A}$ in this case. Having chosen $w_{21} < 0$ we will set all other connections to be excitatory: w_{12}, w_{23}, $w_{32} > 0$. Thus, for satisfying Dale's rule we have chosen a bi-directional 3-chain with inhibitory neuron at one end (figure 8b).

Due to lemma 1 this dynamics f_ρ (27) is now topologically conjugate to that of 8 other parameter vectors $\rho' \in \mathbf{R}^7$ generated again by the basic transformations T_k, $k = 1, 2, 3$ of equations (5), (6). Furthermore, the dynamics of this module is again essentially a 2-dimensional one, because now the neurons 1 and 3 are synchronized in a general sense [22]; i.e. their activities are related by the equation

$$a_3(t) = \theta_3 + \frac{w_{32}}{w_{12}}(a_1(t) - \theta_1) \;. \tag{28}$$

This can be seen, for instance, in figure 15, where the projection onto the (o_1, o_3)-subspace of a chaotic attractor appears to be 1-dimensional. Although the dynamic of this module is again 2-dimensional, its dynamics seems to be more complex than that of the last module (23) as will be discussed next.

The point $a^* = (0, 0, 0)$ is always a fixed point of the dynamics (27), iff the parameters satisfy $-2\theta_1 = w_{12}$, $-2\theta_2 = w_{21} + w_{23}$, and $-2\theta_3 = w_{32}$. It becomes non-hyperbolic if one of the eigenvalues

$$\lambda_{2,3}(0) = \pm\frac{1}{4}\sqrt{w_{12}w_{21} + w_{23}w_{32}}$$

has modulus 1. The first eigenvalue $\lambda_1(0)$ is always zero.

To study dynamically interesting parameter domains we now choose competing even and odd loops, i.e., $w_{12} \cdot w_{21} < 0$ and $w_{23} \cdot w_{32} > 0$. The appearance of periodic and chaotic parameter domains is revealed, for instance, in figure 12 for the (w_{23}, w_{21})-parameter subspace. Following Dale's rule the other five parameters are fixed conveniently as follows: $\theta_1 = -3$, $\theta_2 = 3.95$, $\theta_3 = -7$, $w_{12} = w_{32} = 8$.

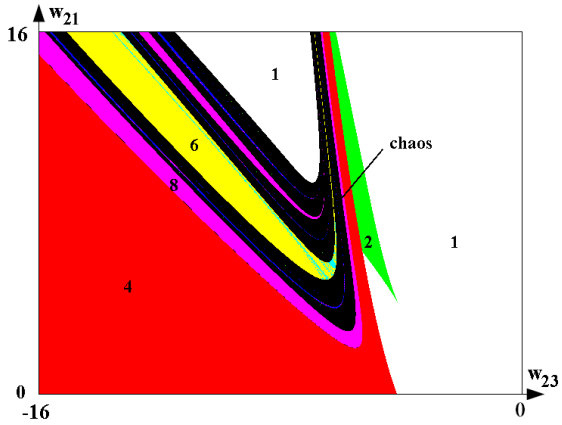

Figure 12: 3-chain 4.2: Iso-periodic plot in the (w_{21}, w_{23})-parameter subspace with fixed parameters $w_{12} = w_{32} = 8$, $\theta_1 = -3$, $\theta_2 = 3.95$, $\theta_3 = -7$.

We will not describe the dynamics as detailed as for the 2-module: we observe mainly the same features: periodic and quasi-periodic attractors, period doubling routes to chaos, etc. What is new for this 3-neuron module is its even greater complexity: Here we not only observe one period-doubling sequence, but coexisting period-doubling routes to chaos leading to coexisting chaotic attractors. For example figure 12 indicates period-doubling to chaos (black domain) starting from period-4 orbit attractors indicated by the red domain. In fact, simulations show, that the period-4 attractor bifurcates into two period-8 attractors, inducing two separated routes to chaos.

The same holds for the period-6 domain (yellow) of figure 12 included in the chaotic region: It stands for coexisting period-3 and period-6 attractors bifurcating along different routes to chaos. After staying separate for a while, these coexisting chaotic attractors experience an *attractor merging crisis* at specific parameter values; i.e. they end up in one attractor.

For $w_{21} > 4$ there is a cusp shaped region (green) of period-2 attractors that, for decreasing w_{23} undergo period-doubling to chaos. All these different routes to chaos coexist in parameter domains around $w_{23} = 7$ and $w_{21} > 8$.

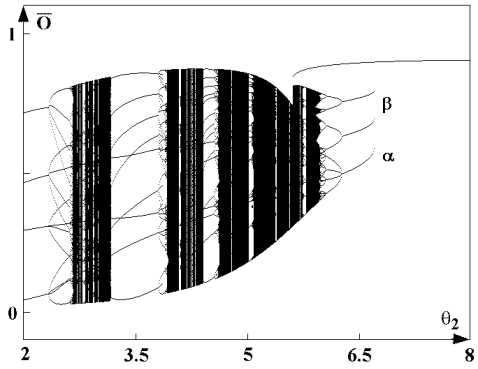

Figure 13: 3-chain 4.2: Bifurcation sequence for θ_2 and fixed parameters $-w_{21} = w_{23} = w_{12} = w_{32} = 8$, $\theta_1 = -3$, $\theta_3 = -7$.

This complicated dynamical properties are clearly visible in the bifurcation diagram of figure 13 for θ_2. Here the weights are fixed at $-w_{21} = w_{23} = w_{12} = w_{32} = 8$, and bias terms at $\theta_1 = -3$, $\theta_3 = -7$. Starting with $\theta_2 = 8$ we have a global fixed point attractor. With θ_2 decreasing, at $\theta_2 = 6.72$ a period-2 (marked by β) and a fixed point attractor (marked by α) appear in addition. At $\theta_2 = 6.23$ coexisting period-doubling routes to chaos start with the period-2 attractor bifurcating into a period-4 orbit and the fixed point attractor bifurcating with a strong resonance of order 4 also into period-4 attractors. The upper sequence (starting from the period-2 orbit) vanishes together with the fixed point attractor at $\theta_2 = 5.63$ and only the lower sequence remains, ending up in a period-4 orbit around $\theta_2 = 2.35$. These period-4 attractors appear through a strong resonance bifurcation of order 4 from a global fixed point at $\theta_2 = -0.58$.

We notice, that for this configuration there exists a general hysteresis phenomenon over the interval $5.63 < \theta_2 < 6.72$, where a whole period-doubling route to chaos and a fixed point attractor is involved: Crossing this hysteresis interval with θ_2 increasing, only the reverse bifurcation sequence to the fixed point is visible; crossing it with θ_2 decreasing, only the fixed point attractor appears. The bifurcation sequence in between stays invisible as well as the hidden bifurcation sequence belonging to the period-2 orbit.

The two chaotic attractors coexisting with the fixed point attractor in this hysteresis domain for $\theta_2 = 5.65$ in figure 13 are shown in figure 14 in a pseudo orbit representation, where $\overline{o}(t+1)$ is plotted against $\overline{o}(t)$, and $\overline{o}$ denotes again the averaged module output $\overline{o} := \frac{1}{3}\sum_{i=1}^{3} o_i$. In figure 14 the projections of these attractors onto the three subspaces $(o_1, o_2$, $((o_1, o_3)$, (o_2, o_3): One of the chaotic attractor has the form of two straight lines, the

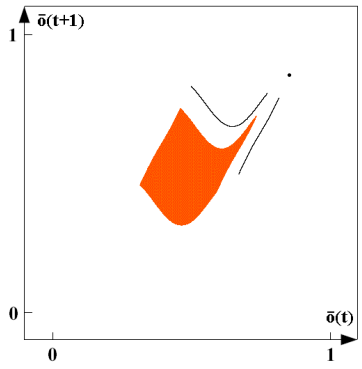

Figure 14: 3-chain 4.2: First return map of two chaotic attractors coexisting with one fixed point attractor for parameter values $-w_{21} = w_{23} = w_{12} = w_{32} = 8$, $\theta_1 = -3$, $\theta_2 = 5.65$, $\theta_3 = -7$.

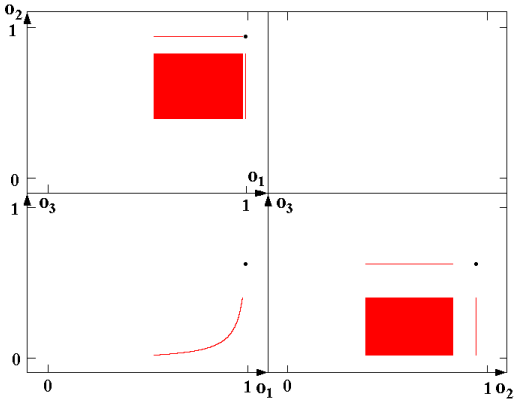

Figure 15: 3-chain 4.2: Same attractors as in figure 14, but shown in terms of the three projections.

other one comes as a rectangle; the fixed point is magnified. Parameters are again $-w_{21} = w_{23} = w_{12} = w_{32} = 8$, $\theta_1 = -3$, $\theta_2 = 5.65$, $\theta_3 = -7$. It is clearly seen from these projections that the attractors live on a 2-dimensional sub-manifold.

4.3 Bi-directional 3-ring with one inhibitory neuron

The third candidate for complex dynamics is a 3-neuron module corresponding to a bi-directional ring (figure 8c). Its discrete dynamics is given by a nine parameter family of maps $f_\rho : \mathbf{R}^3 \to \mathbf{R}^3$ defined by

$$\begin{aligned} a_1(t+1) &:= \theta_1 + w_{12}\,\sigma(a_2(t)) + w_{13}\,\sigma(a_3(t))\,, \\ a_2(t+1) &:= \theta_2 + w_{21}\,\sigma(a_1(t)) + w_{23}\,\sigma(a_3(t))\,, \\ a_3(t+1) &:= \theta_3 + w_{31}\,\sigma(a_1(t)) + w_{32}\,\sigma(a_2(t))\,. \end{aligned} \tag{29}$$

To expect complex dynamical behavior for this module there should be a inhibitory neuron involved, neuron 1 say; i.e. $w_{21},\ w_{31} < 0$. The other neurons are chosen to be excitatory. Then the second and third row of the linearization Df_ρ can satisfy condition (7) of our complex dynamics criterion. For instance for neuron 3 we get

$$w_{31}\sigma'(a_1) + w_{32}\sigma'(a_2) \;= 0\,. \tag{30}$$

The chaos condition (11) for the third component reads

$$Inv_3 = w_{31}w_{13}\sigma'(a_1) + w_{23}w_{32}\sigma'(a_2) \;= 0\,,$$

which can be satisfied because in addition to $w_{31} < 0$ we have chosen $w_{13},\ w_{32},\ w_{23} > 0$.

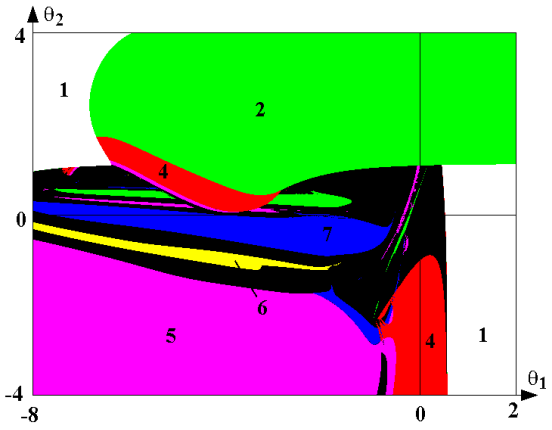

Figure 16: 3-ring 4.3: Iso-periodic plot in the (θ_1, θ_2)-parameter subspace with fixed parameters $-w_{21} = -w_{31} = w_{23} = w_{12} = w_{32} = w_{13} = 8$, $\theta_3 = 5.5$.

The dynamics of this module, different to that of the other 3-neuron modules discussed above, is in general 3-dimensional. Furthermore, due to

lemma 1, the dynamics f_ρ (29) is again topologically conjugate to that of 8 other parameter vectors $\rho' \in \mathbf{R}^9$ generated by the transformations T_k, $k = 1, 2, 3$ of equations (5), (6).

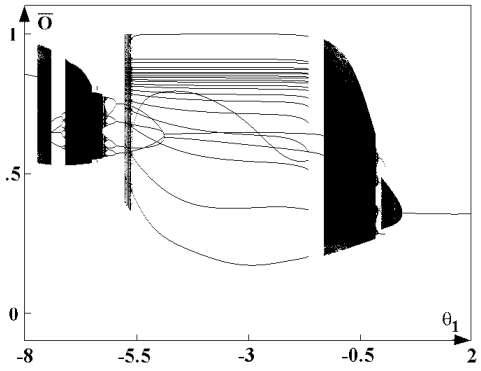

Figure 17: 3-ring 4.3: A bifurcation diagram for θ_1 with parameters $\theta_2 = 1$, $\theta_3 = 5.5$, $-w_{21} = -w_{31} = w_{23} = w_{12} = w_{32} = w_{13} = 8$ fixed.

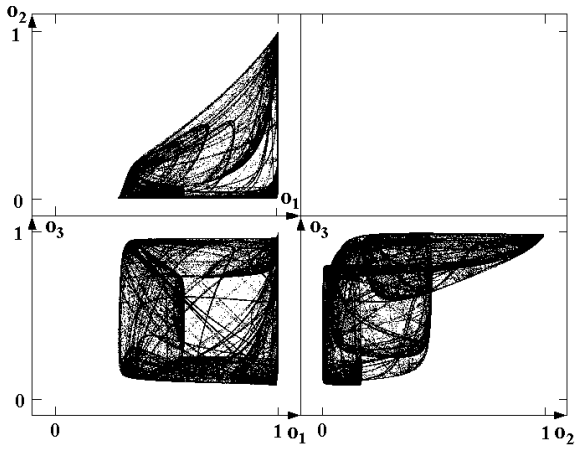

Figure 18: 3-ring 4.3: Three projections of an chaotic attractor at parameter values $-w_{21} = -w_{31} = w_{23} = w_{12} = w_{32} = w_{13} = 8$, $\theta_1 = -1.75$, $\theta_2 = 0$, $\theta_3 = 5.5$.

To get an impression of the dynamical complexity of this 3-neuron module, we may take a look at the iso-periodic plot in the (θ_1, θ_2)-subspace in figure 16. Obviously we have to expect a complex dynamical behavior again with coexisting attractors of different kind. This can be read from the overlapping regions in figure 16 around $\theta_1 = -4$, $\theta_2 = 4$. A bifurcation sequence in this domain will reveal further details, as , for instance, the one shown

in figure 17. There we observe quasiperiodic attractors bifurcating from a fixed pint attractor at around $\theta_1 = 0.46$. For a short interval these attractors coexist with period-5 attractors (around $\theta_1 = 0$). With θ_1 further decreasing, a chaotic domain is entered which ends around $\theta_1 = -1.31$. Then a domain with period-2 attractors follows up to $\theta_1 = -4.88$, where a period-doubling route to chaos starts. Over the long interval $-5.77 < \theta_1 < -1.64$ together with the period-2 attractors there exist period-21 attractors.

That the dynamics (29) is a genuine 3-dimensional one can be seen in figure 18, where three projections of a chaotic attractor are shown. This attractor exists for parameter values $-w_{21} = -w_{31} = w_{23} = w_{12} = w_{32} = w_{13} = 8$, $\theta_1 = -1.75$, $\theta_2 = 0$, $\theta_3 = 5.5$.

4.4 Complex dynamics, no chaos

Finally we want to introduce two 3-neuron modules for which apparently no chaotic attractors exist, although there are higher-periodic attractors and interesting bifurcation sequences. The first example starts again with the bi-direction 3-ring (29) but now with one of the weights equal to zero, $w_{23} = 0$ say. Then the complexity condition (30) for the third unit can still be satisfied but the chaos condition can not be satisfied because it now reads

$$Inv_1(a) = w_{31} w_{13} \sigma'(a_1) \sigma'(a_3) < 0 \ , \quad a \in \mathcal{A} \ ,$$

which is strictly negative.

The second example is given by a uni-directional 3-ring with one self-inhibitory neuron. Its dynamics is given by the equation

$$\begin{aligned} a_1(t+1) &:= \theta_1 + w_{11}\, \sigma(a_1(t)) + w_{13}\, \sigma(a_3(t)) \ , \\ a_2(t+1) &:= \theta_2 + w_{21}\, \sigma(a_1(t)) \ , \\ a_3(t+1) &:= \theta_3 + w_{32}\, \sigma(a_2(t)) \ . \end{aligned} \tag{31}$$

The satisfiable complex dynamics condition (7) for the first component is here given by the equation

$$w_{11}\, \sigma'(a_1) + w_{13}\, \sigma'(a_3) = 0 \ ,$$

i.e. with $w_{11} w_{13} < 0$ and, for instance, $w_{11} < 0$. But the chaos condition can not be satisfied because it reads

$$Inv_1(a) = w_{11}^2 (\sigma')^2(a_1) > 0 \ , \quad a \in \mathcal{A} \ ,$$

which is strictly positive.

5 Discussion

From the very simple example networks discussed in this paper there are some lessons to learn about artificial recurrent networks: First, from the point of view of dynamical systems theory, the sigmoidal transfer functions of these neural networks provide an interesting nonlinearity into these systems. Already for the simple chaotic 2-module many dynamical effects can be studied just in this one system alone; i.e. there are period doubling routes to chaos, like in the quadratic map; there are Neimark-Sacker bifurcations from fixed point attractors to attractors with higher periodicity as well. All kinds of attractors can be observed: fixed points, higher periods, quasi-periodic and chaotic attractors. Furthermore, for one and the same parameter vector attractors of different type can exist simultaneously, even different chaotic attractors.

This co-existence of attractors often gives rise to a so-called *generalized hysteresis* effect. In the simplest case this corresponds to a parameter domain where two fixed point attractors co-exist with an unstable fixed point. Passing forward and backward over this domain makes the system switch between these different stationary states at different parameter values. As was shown in figures 14 and 15, even dynamic attractors can co-exist and the corresponding generalized hysteresis effect may serve as a kind of *short-term memory of dynamical behaviors*. Much in the same way as the usual hysteresis effect serves as a memory of stationary states in magnets or computer chips. Thinking of attractors as representatives of mental or behavior relevant states would explain for instance the flipping of the ambiguous figures in the visual domain or hysteresis effects in finger tapping [15] or bimanual coordination experiments [14].

It should be remarked that with respect to cognitive processes attractors will be always considered as representatives of a class of different dynamical solutions or trajectories. In fact, as part of cognitive systems the dynamics of the system will hardly ever be that of an attractor because these systems are permanently driven by stimulating external sensor signals or by internal stimuli coming from other parts of the cognitive system. Thus, what should be considered relevant for the discussion or interpretation of "cognitive dynamics" are the basins of attraction of these systems; and the properties of basin boundaries may be more relevant for the understanding than the exact "shape" of the representing attractor.

With respect to higher information processing or cognitive abilities these dynamical neural networks represent a practically unlimited reservoir of possible behaviors. They can be coupled in very different ways, using excitatory as well as inhibitory connections between the neurons of subsystems. Es-

pecially if recurrent couplings of such neuromodules are involved one can observe new or more "complex" dynamical properties in the coupled system. This phenomenon of *emergent dynamics* is the basis for hopes that it should be possible to generate more powerful systems from specific coupling schemes of "simple" neuromodules. At some point even "cognitive" abilities may emerge (the flip from quantity to quality). At the same time, these nonlinear dynamical effects are an absolute drawback for design or engineering approaches to these kind of systems. In general there never can be construction rules for this approach to cognitive systems, at least not at the moment, where there is no theory available to predict the behavior of these coupled systems.

A question often heard is the following: "Now you have complex dynamics, even chaos; so what?" There may be chaos in the brain as stated years ago by Skarda and Freeman [31], and if one looks for chaos in biological brains it would be a surprise if one will *not* find signals indicating chaotic dynamics in this very high-dimension, highly connected recurrent network with inhibitory and excitatory signal lines. But even if so, the functional role is still debatable and an open problem. The point we want to make in favour of chaotic neuromodules here is, that they provide the richest reservoir of possible dynamical features which are accessable by tuning the parameters correctly. If one needs stationary states, well you can find them, if you need a specific periodic orbit, you will find it, if you want chaos for representing "emptiness", a rest state or a specific function, its to your proposal. In this sense, chaotic modules are just powerful and versatile building blocks for systems which have to have a large reservoir of different behaviors at their disposal to survive in a changing environment.

The choice of specific attractors or attractor combination is of course up to a kind of adaptive self-organizing process on the parameter space of networks, which one may call *learning*. Learning is still a challenging problem for neural networks of a general recurrent type. Thinking of these networks as controllers for the behavior of biological or artificial autonomous systems makes the problem even more challenging because there is no way to determine the correct function of a subsystem during the process generating a goal oriented behavior. One way to get an idea about module function and the coupling of neuromodules is to study them as evolved controllers for the behavior of robots. This is done for instance in [26].

References

[1] Abeles, M. (1991), *Corticonics*, Cambridge University Press, Cambridge.

[2] Abraham, R. H., Gardini, L. and Mira, C. (1997), *Chaos in Discrete Dynamical Systems*, Springer-Verlag, New York.

[3] Arbib, M A., Érdi, P., and Szentágothai, J (1998), *Neural Organization - Structure, Function, and Dynamics*, MIT Press, Massachusetts.

[4] An der Heiden, U. (1980) *Analysis of Neural Networks* (Lecture Notes in Biomathematics **35**, Springer Verlag, Berlin.

[5] Beer, R. D. (1995), On the dynamics of small continuou-time recurrent networks, *Adaptive Behavior*, **3**, 471–511.

[6] Blum, E. K., and Wang, X. (1992), Stability of fixed points and periodic orbits and bifurcations in analog neural networks, *Neural Networks*, **5**, 577–587.

[7] Borisyuk, R. M., and Kirillov, A. (1992), Bifurcation analysis of neural network model, *Biological Cybernetics*, **66**, 319–325.

[8] Botelho, F. (1999), Dynamical features simulated bby recurrent neural networks, *Neural Networks*, **12**, 609–615.

[9] Buzsáki, G., Llinás, R., Singer, W., Berthoz, A., and Christen, Y. (Eds.) (1994) *Temporal Coding in the Brain*, Springer, Berlin.

[10] Chapeau-Blondeau, F., and Chauvet G. (1992), Stable, oscillatory, and chaotic regimes in the dynamics of small neural networks with delay, *Neural Networks*, **5**, 735–743.

[11] Douglas, R. J., Martin, K. A. C., and Whitteridge, D. (1989), A canonical microcircuit for neocortex, *Neural Computation*, **1**, 480 – 488.

[12] Duke, W., and Pritchard, W. S. (Eds.) (1991), *Proceedings of the Conference on Measuring Chaos in the Human Brain*, World Scientific, Singapore.

[13] Elbert, T., Ray, W.J., Kowalik, Z.J., Skinner, J.E., Graf, K.E., and Birbaumer, N. (1994), Chaos and physiology: Deterministic chaos in excitable cell assemblies, *Physiological Review, American Physiological Society*, **74**, 1–47.

[14] Kelso, J. A. S. (1995), *Dynamic Patterns - The Self-Organization of Brain and Behavior*, MIT Press, Cambridge.

[15] Kelso, J. A. S., DelColle, J. D., and Schner, G. (1990), Action-perception as a pattern formation process, in: Jeannerod, M. (Ed.), *Attention and Performance XIII*, pp. 139-169, Hillsdale, NJ: Erlbaum.

[16] Klotz, A. and Brauer, K. (1999), A small-size neural network for computing with strange attractors, *Neural Networks*, **12**, 601–607.

[17] Mackey, M. C., and an der Heiden, U. (1984), The dynamics of recurrent inhibition, *J. Math. Biol.*, **19**, 211–225.

[18] Marcus, C. M., and Westervelt R. M. (1989), Dynamics of iterated-map neural networks, *Phys. Rev.*, **A40**, 501-504.

[19] Pakdaman, K., Grotta-Ragazzo, C., Malta, C. P., Arino, O., and Vibert, J. F. (1998), Effect of delay on the boundary of the basins of attraction in a system of two neurons, *Neural Networks*, **11**, 509–519.

[20] Pantev, C., Elbert, T., and Lutkenhöhner, B. (Eds.) (1995), *Oscillatory event-related brain dynamics*, Plenum, London.

[21] Pasemann, F. (1993), Dynamics of a single model neuron, *International Journal of Bifurcation and Chaos*, **2**, 271-278.

[22] Pasemann, F., and Wennekers, T. (2000), Generalized and partial synchronization of coupled neural networks, *Network: Computation in Neural Systems*, **11**, 41–61.

[23] Pasemann, F. (1995), Characteristics of periodic attractors in neural ring networks, *Neural Networks*, **8**, 421-429.

[24] Pasemann, F. (1995), Neuromodules: A dynamical systems approach to brain modelling, in H. Herrmann, E. Pöppel, D. Wolf (Eds.), *Supercomputing in Brain Research - From Tomography to Neural Networks*, (pp. 331–347). Singapore: World Scientific.

[25] Pasemann, F. (1998), Structure and Dynamics of Recurrent Neuromodules, *Theory in Biosciences*, **117**, 1–17.

[26] Pasemann, F., Steinmetz, U., and Hülse, M. (2001), Robot control and the evolution of modular neurodynamics, MPI-MIS Preprint ???/2001, and *Theory in Biosciences*, to appear.

[27] Port, R., and van Gelder, T. (Eds.) (1995), *Mind as Motion: Explorations in the Dynamics of Cognition*, Cambridge MA: MIT Press.

[28] Poston, T., and Stewart, I. (1978) *Catastrophe Theory and its Applications*, Pitman, London.

[29] Shepherd, G. M. (ed.) (1990) *The Synaptic Organization of the Brain Cortex*, Ocford Univ. Press, New York.

[30] Renals, S., and Rohwer, R. (1990), A study of network dynamics, *Journal of Statistical Physics*, **58**, 825–848.

[31] Skarda, C.A., and Freeman W.J. (1987), How brains make chaos in order to make sense of the world, *Behavioural Brain Science*, **10**, 161–195.

[32] Szentagothai, J. (1983), The modular architectonic principle of neural centers, *Rev. Physiol. Biochem. Pharmacol.*, **98**, 11–61.

[33] Thom, R. (1975) *Structural Stability and Morphogenesis*, Benjamin, Reading.

[34] Thompson, J. M. T., and Stewart, H. B. (1986), *Nonlinear Dynamics and Chaos*, Chichester: John Wiley.

[35] Tino, P., Horne, B. G., and Giles, C. L. (2001), Attractive periodic sets in discrete time recurrent networks, *Neural Computation*, **13**, 1379–1414.

[36] Traub, R. D., and Miles, R. (1991), *Neuronal Networks of the Hippocampus*, Cambridge University Press, New York.

[37] Wang, X. (1991) Period-doublings to chaos in a simple neural network: An analytic proof, *Complex Systems*, **5**, 425–441.

[38] White, E. L. (1989), *Cortical Circuits: Synaptic Organization of the Cerebral Cortex Structure, Function and Theory*, Birkhäuser, Boston.

[39] Wilson, H. R., and Cowan,J. D. (1972), Excitatory and inhibitory interactions in localized populations of model neurons, *Biophys. J.*, **12**, 1–23.